THE JOURNAL OF BIOLOGICAL CHEMISTRY VOL. 290, NO. 51, pp. 30616–30623, December 18, 2015

Molecular Basis of Regulating High Voltage-Activated Calcium Channels by *S*-Nitrosylation*

Received for publication, August 12, 2015, and in revised form, October 16, 2015 Published, JBC Papers in Press, October 27, 2015, DOI 10.1074/jbc.M115.685206

Meng-Hua Zhou, Alexis Bavencoffe, and Hui-Lin Pan[1]

From the Department of Anesthesiology and Perioperative Medicine, Center for Neuroscience and Pain Research, The University of Texas MD Anderson Cancer Center, Houston, Texas 77030

Nitric oxide (NO) is involved in a variety of physiological processes, such as vasoregulation and neurotransmission, and has a complex role in the regulation of pain transduction and synaptic transmission. We have shown previously that NO inhibits high voltage-activated Ca^{2+} channels in primary sensory neurons and excitatory synaptic transmission in the spinal dorsal horn. However, the molecular mechanism involved in this inhibitory action remains unclear. In this study, we investigated the role of *S*-nitrosylation in the NO regulation of high voltage-activated Ca^{2+} channels. The NO donor *S*-nitroso-*N*-acetyl-DL-penicillamine (SNAP) rapidly reduced N-type currents when Cav2.2 was coexpressed with the Cavβ1 or Cavβ3 subunits in HEK293 cells. In contrast, SNAP only slightly inhibited P/Q-type and L-type currents reconstituted with various Cavβ subunits. SNAP caused a depolarizing shift in voltage-dependent N-type channel activation, but it had no effect on Cav2.2 protein levels on the membrane surface. The inhibitory effect of SNAP on N-type currents was blocked by the sulfhydryl-specific modifying reagent methanethiosulfonate ethylammonium. Furthermore, the consensus motifs of *S*-nitrosylation were much more abundant in Cav2.2 than in Cav1.2 and Cav2.1. Site-directed mutagenesis studies showed that Cys-805, Cys-930, and Cys-1045 in the II-III intracellular loop, Cys-1835 and Cys-2145 in the C terminus of Cav2.2, and Cys-346 in the Cavβ3 subunit were nitrosylation sites mediating NO sensitivity of N-type channels. Our findings demonstrate that the consensus motifs of *S*-nitrosylation in cytoplasmically accessible sites are critically involved in post-translational regulation of N-type Ca^{2+} channels by NO. *S*-Nitrosylation mediates the feedback regulation of N-type channels by NO.

High voltage-activated (HVA) Ca^{2+} channels play obligatory roles in diverse physiological functions, including regulation of gene expression, synaptic transmission, and muscle contraction. These channels are heteromeric protein complexes composed of α_1, β, and $\alpha_2\delta$ subunits (1, 2). The α_1 subunit (Cavα_1) contains the channel pore and is the principal component of HVA Ca^{2+} channels. Both Cavα_1 and cytosolic auxiliary β subunits (Cavβ) carry out essential gating functions (1, 3, 4). Cavα_1 has the most drug-binding sites of the subunits, whereas Cavβ is essential for regulating the surface expression of the channel complex (1).

There exist several types of HVA Ca^{2+} channels, including L-, N-, P/Q-, and R-types. L-type Ca^{2+} channels are not only present in cardiac and smooth muscles but also expressed in neurons and endocrine cells where they regulate a multitude of processes, including the release of hormones and neurotransmitters and gene expression (5, 6). N-type channels are distributed in the brain and peripheral nervous system and are the major subtypes present in nociceptive dorsal root ganglion (DRG)[2] neurons (7–10). P/Q-type channels are involved in neurotransmitter release at synaptic terminals (11, 12). The Cavβ subunits (Cavβ1-Cavβ4) are abundantly expressed in excitable tissues such as the brain, heart, and muscles. Cavβ3 is the predominant partner of Cav2.2 (N-type), and Cavβ4 is the most prevalent partner of Cav2.1 (P/Q-type) in the brain (3, 13). HVA Ca^{2+} channels are essential for the nociceptive transmission (14, 15), and changes in HVA Ca^{2+} channel properties in DRG neurons may be involved in the development of chronic neuropathic pain (16–18).

Nitric oxide (NO) plays a complex role in the modulation of pain. Although some studies suggest that NO is pro-nociceptive (19, 20), NO can also reduce pain and nociceptive transmission (21–23). Indeed, our previous study has shown that NO inhibits HVA Ca^{2+} channel currents in DRG neurons and attenuates excitatory synaptic transmission in the spinal dorsal horn (24). However, the molecular mechanism underlying this inhibitory action is still unclear. NO exerts ubiquitous signaling via post-translational modification of cysteine residues, a reaction termed *S*-nitrosylation. Because nitrosothiols are exceptionally labile because of their reactivity with intracellular reducing reagents such as ascorbic acid, *S*-nitrosylation functions as a reversible post-translational modification analogous to phosphorylation. *S*-Nitrosylation is involved in regulation of NMDA receptors (25) and ryanodine receptor/Ca^{2+} release channels (26). In DRG neurons, NO-induced HVA Ca^{2+} channel inhibition is resistant to the guanylate cyclase inhibitor (24). However, *N*-ethylmaleimide, a specific alkylating agent of cysteine sulfhydryl, prevents the inhibitory effect of the NO precursor L-arginine and the NO donor *S*-nitroso-*N*-acetyl-DL-penicillamine (SNAP) on HVA Ca^{2+} channels (24). Thus, NO likely inhibits HVA Ca^{2+} channels through cGMP-indepen-

* This work was supported, in whole or in part, by National Institutes of Health Grants HL077400 and NS073935 and the N. G. and Helen T. Hawkins endowment (to H.-L. P.). The authors declare no conflict of interest.

[1] To whom correspondence should be addressed: Unit 110, 1515 Holcombe Blvd., Houston, TX 77030. Tel.: 713-563-7467; Fax: 713-794-4590; E-mail: huilinpan@mdanderson.org.

[2] The abbreviations used are: DRG, dorsal root ganglion; HVA, high voltage-activated; SNAP, *S*-nitroso-*N*-acetyl-DL-penicillamine; MTSEA, methanethiosulfonate ethylammonium.

dent pathways such as the nitrosylation of free sulfhydryl groups of cysteine residues.

In this study, we determined the role of *S*-nitrosylation in the effects of NO on various types of reconstituted HVA Ca^{2+} channels. We present new molecular evidence showing cysteine modification as a distinct mechanism for regulation of N-type channels by NO.

Experimental Procedures

Cell Culture and Transfection—Human embryonic kidney (HEK) 293 cells were cultured in Dulbecco's modified Eagle's medium (Gibco/Life Technologies) supplemented with 10% fetal bovine serum (Sigma) at 37 °C in 5% CO_2. For transfection experiments, 1.2×10^4 cells were plated on poly-D-lysine-coated coverslips in each well of a 24-well plate. After 24 h, we used PolyJet DNA In Vitro transfection reagent (SignaGen Laboratories, Gaithersburg, MD) to transiently transfect the cells with various combinations of Cavα_1 (Cav1.2, Cav2.1, or Cav2.2), $\alpha_2\delta1$, and Cavβ (Cavβ1-Cavβ4) subunits. The sources of cDNAs for rat Cavα_1, $\alpha_2\delta1$, and Cavβ subunits were reported previously (27, 28). A Cav2.2-V5 construct was made by inserting a rat Cav2.2 fragment into a pCDNA6 V5-FLAG vector using an In-Fusion HD Cloning Kit (Clontech, Palo Alto, CA). The pCDNA6 V5-FLAG vector was kindly provided by Dr. Jiusheng Yan (MD Anderson Cancer Center, Houston, TX). We cotransfected HEK293 cells with multiplasmids of HVA Ca^{2+} channels at a 1:1:1 ratio and changed the medium after 4 h. Electrophysiological recordings and biochemical assays were performed 48–72 h after transfection.

Electrophysiological Recording—Whole cell patch clamp recordings were performed using an EPC-10 amplifier (HEKA Instruments, Lambrecht, Germany). The whole cell Ca^{2+} currents, carried by barium (I_{Ba}), were recorded using an extracellular recording solution consisting of (in mM) 140 tetraethylammonium chloride, 2 $MgCl_2$, 3 $BaCl_2$, 10 glucose, and 10 HEPES (pH 7.4, osmolarity, 320 mOsm). Electrodes (resistance, 4–6 megaohms) were filled with pipette solution containing (in mM) 120 CsCl, 1 $MgCl_2$, 10 HEPES, 10 EGTA, 4 MgATP, and 0.3 NaGTP (pH 7.2, osmolarity, 300 mosmol). The cell membrane capacitance and series resistance were electronically compensated. Signals were filtered at 1 kHz, digitized at 10 kHz, and acquired using the Pulse program (HEKA Instruments).

SNAP (Abcam, Cambridge, MA) and dithiothreitol (DTT, Sigma) were delivered to the recording chamber by gravity. Methanethiosulfonate ethylammonium (MTSEA) was purchased from Toronto Research Chemicals Inc. (Toronto, ON, Canada).

Cell Surface Protein Isolation and Cav2.2 Surface Expression—HEK293 cells transfected with V5-tagged Cav2.2, Cavβ3, and $\alpha_2\delta1$ were treated with SNAP for 5 min and quickly washed with PBS. Cell surface biotinylation and surface protein isolation were carried out using the cell surface protein isolation kit (Pierce Biotechnology, Rockford, IL) according to the manufacturer's instructions. The surface protein samples were probed with the anti-V5 antibody (1:1,000 dilution; Life Technologies, Grand Island, NY) and Na^+/K^+-ATPase antibody (1:1,000 dilution; EMD Millipore, Billerica, MA) using Western blot analysis. Na^+/K^+-ATPase, a plasma membrane protein, was used as a loading control. The amounts of Cav2.2 proteins were normalized by the protein band of Na^+/K^+-ATPase. The mean value of Cav2.2 protein levels in HEK293 cells treated with the vehicle was defined as 1 (27).

Site-directed Mutagenesis—Point mutations were performed using the QuikChange Site-directed Mutagenesis Kit (Stratagene, Santa Clara, CA) or the In-Fusion HD Cloning Kit (Clontech) according to the manufacturer's instructions.

Data Analysis—The HVA Ca^{2+} current data were analyzed using Origin 8 software (Microcal Software, Northampton, MA). Conductance-voltage (G-V) curves were fitted using the Boltzmann equation, $G/G_{max} = 1/\{1 + \exp[(V_{0.5} - V_m)/k]\}$. $G = I/(V_m - V_{rev})$, where G is the membrane conductance, V_m is the test potential, and V_{rev} is the reversal potential. $V_{0.5}$ is the voltage for 50% activation or inactivation of HVA Ca^{2+} currents, and k is a voltage-dependent slope factor. Western immunoblotting data were quantified by LI-COR Image Studio software (LI-COR Biosciences, Lincoln, NE). We used the Student's t test to compare the SNAP or MTSEA effects on HVA Ca^{2+} currents between two groups. For comparing the differences in the SNAP effects on N-type channel currents between the wild-type and various mutant groups, we used the χ-square test with Yates correction for continuity. Values are given as mean ± S.E., with n indicating the number of cells used for the electrophysiological recording or the number of independent repeats for biochemical experiments. Differences were considered statistically significant if the p value was less than 0.05.

Results

Differential Effects of SNAP on N-type, P/Q-type, and L-type Channels—To determine whether NO differentially inhibits different HVA Ca^{2+} channels, we compared the inhibitory effects of the NO donor SNAP on N-type (Cav2.2), P/Q-type (Cav2.1), and L-type (Cav1.2) channels in HEK293 cells cotransfected with $\alpha_2\delta1$ and different Cavβ (Cavβ1, Cavβ2, Cavβ3, or Cavβ4) subunits. The whole cell I_{Ba} were elicited by a depolarizing pulse to 0 mV for 200 ms from a holding potential of −90 mV. Bath application of 100 μM SNAP caused a rapid and large inhibition of the current amplitude of N-type Ca^{2+} channels reconstituted with Cavβ1 (42.46 ± 7.12%, $n = 7$) or Cavβ3 (33.27 ± 3.28%, $n = 7$; Fig. 1). In contrast, SNAP only slightly inhibited N-type Ca^{2+} channel currents reconstituted with Cavβ2 (9.97 ± 1.84%, $n = 7$) or Cavβ4 (15.20 ± 1.82%, $n = 8$, Fig. 1). Upon SNAP washout, the reduced HVA Ca^{2+} currents often persisted for more than 10 min. However, the inhibitory effect of SNAP on HVA Ca^{2+} currents was rapidly reversed by bath application of the reducing agent DTT (5 mM, Fig. 1*A*) (25, 29). DTT alone had no significant effect on N-type currents (Fig. 1*B*).

Bath application of SNAP produced only a small inhibitory effect on P/Q-type currents in HEK293 cells coexpressing with Cavβ1 (7.95 ± 2.53%, $n = 8$) or Cavβ3 (8.72 ± 1.69%, $n = 6$) and had no significant effect on P/Q-type currents reconstituted with Cavβ2 or Cavβ4 (Fig. 2). Also, SNAP inhibited L-type currents reconstituted with Cavβ1 (15.41 ± 0.87%, $n = 7$) but had no significant effect on L-type currents reconstituted with Cavβ2, Cavβ3, or Cavβ4 (Fig. 2). Thus, compared with P/Q-

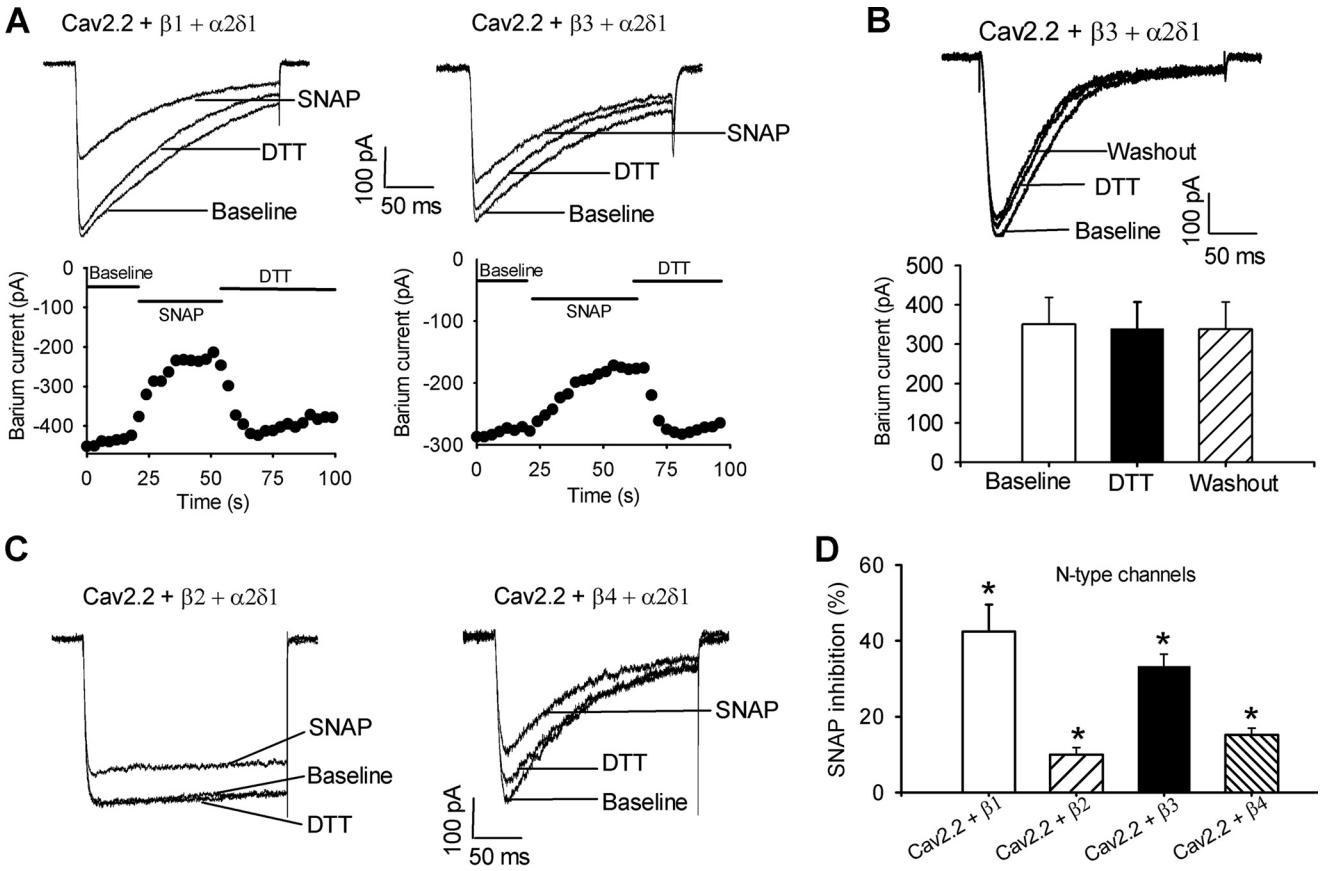

FIGURE 1. **Inhibitory effect of SNAP on N-type channel activity.** *A,* representative current traces and time course show the inhibitory effect of SNAP on N-type channel currents in HEK293 cells cotransfected with Cav2.2, $\alpha_2\delta1$, and Cav$\beta1$ or Cav$\beta3$ subunits. *B,* original recording traces and mead data show the lack of effect of DTT on N-type currents in HEK293 cells cotransfected with Cav2.2, $\alpha_2\delta1$, and Cav$\beta3$ subunits. *C,* original current traces show the SNAP effect on N-type currents in HEK293 cells coexpressing Cav2.2, $\alpha_2\delta1$, and Cav$\beta2$ or Cav$\beta4$ subunits. *D,* summary data show inhibition of N-type channel currents with different Cavβ subunits by 100 μM SNAP. *, $p < 0.05$, compared with the baseline control before SNAP application.

type and L-type channels, N-type channels reconstituted with Cav$\beta1$ or Cav$\beta3$ were much more sensitive to inhibition by NO. In the following experiments, we focused our analysis on NO modulation of N-type channels.

SNAP Causes a Depolarizing Shift of Voltage-dependent Activation of N-type Channels—To examine the SNAP effect on voltage-dependent activation of N-type channels, the membrane potential was held at −90 mV. I_{Ba} currents were elicited by a series of depolarizing pulses for 150 ms from −70 to 50 mV with an interval of 10 mV. HEK293 cells expressing Cav2.2 + $\alpha_2\delta1$ and Cav$\beta1$, Cav$\beta3$, or Cav$\beta4$ subunits were tested. Bath application of 100 μM SNAP caused a significant depolarizing shift of voltage-dependent N-type channel activation (*i.e.* reducing the channel sensitivity to depolarizing voltages) and slightly increased the slope factors when Cav2.2 was coexpressed with Cav$\beta1$ or Cav$\beta3$ (Fig. 3*A*, Table 1). SNAP had no significant effect on voltage-dependent N-type channel activation in HEK293 cells coexpressing Cav2.2, $\alpha_2\delta1$, and Cav$\beta4$ (Fig. 3*A*, Table 1).

The voltage-dependent inactivation of N-type channels was assessed by using a series of pre-pulses from −90 to 10 mV for 500 ms followed by depolarization of the cell to 0 mV for 150 ms (27). Bath application of SNAP had no significant effect on voltage-dependent inactivation of N-type channels in HEK293 cells expressing Cav2.2 + $\alpha2\delta1$ and Cav$\beta1$, Cav$\beta3$, or Cav$\beta4$ (Fig. 3*B*, Table 1).

SNAP Has No Effect on the Membrane Surface Expression of Cav2.2—Because the inhibitory effect of NO on N-type currents may be associated with reduced Cav2.2 trafficking to the plasma membrane, we next analyzed the effect of SNAP on Cav2.2 surface expression. HEK293 cells transfected with V5-tagged Cav2.2, Cav$\beta3$, and $\alpha_2\delta1$ were treated with 100 μM SNAP or vehicle for 5 min. Cell surface proteins were then isolated and subjected to Western blotting analysis. Na^+/K^+-ATPase, a plasma membrane protein, was used as a loading control. The Ca2.2 surface protein levels did not differ significantly between SNAP- and vehicle-treated groups (Fig. 4).

SNAP Inhibits N-type Channels through S-Nitrosylation—The SNAP effect on HVA Ca^{2+} channels in DRG neurons and transfected HEK293 cells is independent of cGMP pathways (24, 29). To determine whether *S*-nitrosylation is involved in the inhibitory effect of NO on N-type currents, we used MTSEA, a membrane-permeable sulfhydryl-specific modifying reagent (25), which can rapidly react with thiols to form mixed disulfides, thereby preventing subsequent *S*-nitrosylation of proteins. HEK293 cells expressing Cav2.2, Cav$\beta3$, and $\alpha_2\delta1$ subunits were pretreated with 2.5 mM MTSEA for 1 min before whole cell recordings. Treatment with MTSEA alone did not

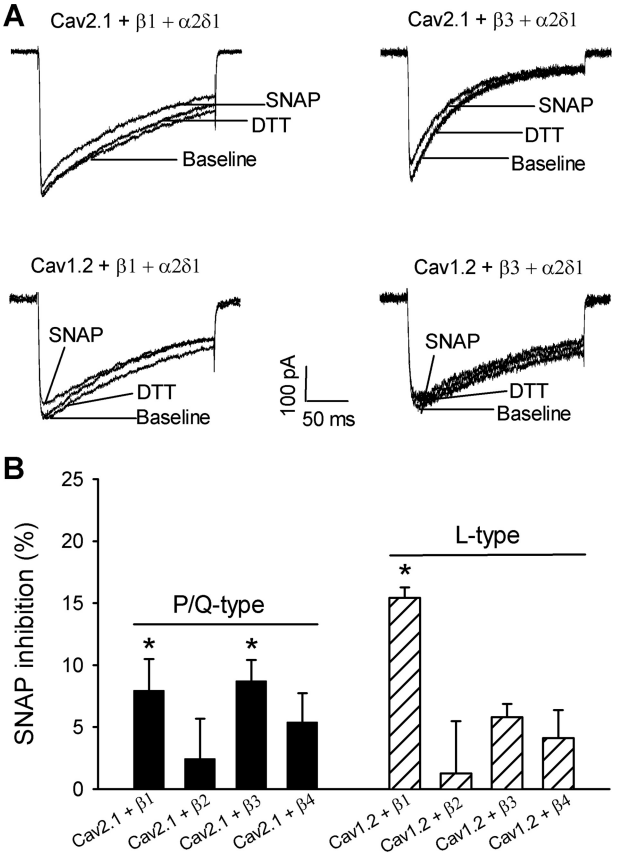

FIGURE 2. **Inhibitory effect of SNAP on P/Q-type and L-type Ca^{2+} channel activity.** *A,* original current traces show the inhibitory effect of SNAP on P/Q-type and L-type channel currents in HEK293 cells cotransfected with Cav2.1 (or Cav1.2), $\alpha_2\delta1$, and Cav$\beta1$ or Cav$\beta3$ subunits. *B,* summary data show inhibition of P/Q-type and L-type I_{Ba} currents by 100 μM SNAP. *, $p < 0.05$, compared with the baseline before SNAP application.

significantly change the amplitude of N-type currents. MTSEA treatment completely blocked the inhibitory effect of 100 μM SNAP on the amplitude of N-type channels (Fig. 5). These results suggest that NO inhibits N-type channels through *S*-nitrosylation.

Intracellular Cysteine Residues of N-type Channels Are Involved in S-Nitrosylation Modification—Our results with the sulfhydryl-specific modifying reagent indicate that NO may interact with cysteine residues to produce its effects on N-type channels. We next used site-directed mutagenesis to identify the possible cysteine residues involved in *S*-nitrosylation modification of N-type channels by NO. We inspected amino acid sequences of Cavα_1 and Cavβ subunits and searched for the candidate *S*-nitrosylation sites. According to a previous report (30), cysteine (Cys) residues followed by glutamic acid (Glu) or aspartic acid (Asp) are the critical sites (*i.e.* the consensus motif of *S*-nitrosylation) involved in NO redox reactions. In N-type channels, there are seven CD/CE pairs: two (Cys-277 and Cys-1688) in the pore loops, three (Cys-805, Cys-930, and Cys-1045) in the II-III intracellular loop, and the remaining two (Cys-1835 and Cys-2145) in the C terminus of the channel (Fig. 6*A*). In contrast, there is only one CD pair in P/Q-type channels (Fig. 6*B*), and there are three CD/CE pairs in L-type channels (Fig. 6*C*).

Sequence alignment analysis showed that the positions of CE pairs in Cavβ subunits are much more conserved than those in Cavα_1 subunits. Cav$\beta1$, Cav$\beta2$, and Cav$\beta4$ subunits have two CE pairs: one in the SH3 domain and the other in the GK domain. For the Cav$\beta3$ subunit, only one CE pair (Cys-346) exists in the GK domain. Because the Cavβ_3 subunit is the predominant partner of Cav2.2 in neurons (13, 28), in the following experiments, we attempted to identify the critical cysteine residues in both Cav2.2 and Cav$\beta3$ subunits involved in *S*-nitrosylation modifications using site-directed mutagenesis.

We mutated the seven cysteine residues individually on the Cav2.2 subunit as well as Cys-346 on the Cav$\beta3$ subunit to alanine. Mutating two cysteine residues (Cys-277 and Cys-1688) in the pore loop of Cav2.2 largely diminished the I_{Ba} currents in HEK293 cells. The maximum current amplitudes produced by C277A and C1688A were 43.92 $\pm$ 16.00 pA ($n = 7$) and 29.21 $\pm$ 3.69 pA ($n = 8$), respectively. Nevertheless, mutating other cysteine residues in Cav2.2 produced wild-type-like N-type currents. In HEK293 cells coexpressing Cavβ_3 + $\alpha_2\delta1$ and C805A, C930A, C1835A, or C2145A mutant of Cav2.2, the inhibitory effect of SNAP on N-type currents was diminished (Fig. 7, Table 2). In HEK293 cells coexpressing Cav$\beta3$, $\alpha_2\delta1$, and the C1045A mutant, the inhibitory effect of SNAP on N-type currents was reduced by about 60% compared with that in wild-type Cav2.2 (Fig. 7, Table 2).

In contrast, mutating Cys-1065, a non-predicted cysteine residue in the II-III intracellular loop, to alanine did not significantly alter the inhibitory effect of SNAP (Fig. 7*B*, Table 2). Furthermore, SNAP had no significant effect on voltage-dependent activation or inactivation of N-type currents reconstituted with the C805A or C930A in HEK293 cells (Fig. 8, Table 1).

Mutating Cys-346 to alanine in the Cav$\beta3$ subunit generated wild-type-like N-type currents in HEK293 cells coexpressing Cav2.2 and $\alpha_2\delta1$. However, the inhibitory effect of SNAP on N-type currents reconstituted with the C346A mutant was reduced by about 50% compared with that in wild-type Cav$\beta3$ (16.02 $\pm$ 3.13% *versus* 32.09 $\pm$ 3.21%; Fig. 7, Table 2). Taken together, our findings reveal that NO inhibits N-type channels through *S*-nitrosylation of intracellular cysteine residues in both α_1 and Cavβ subunits.

Discussion

NO is a pleiotropic cell signaling molecule that controls diverse biological processes. *S*-Nitrosylation is the covalent modification of a protein cysteine thiol by an NO group to generate an *S*-nitrosothiol, which can occur rapidly without the action of any enzymes (25, 31, 32). In the cardiovascular system, *S*-nitrosylation seems to be involved in post-translational modification of several ion channels, including Nav1.5, L-type channels, Kv1.5, and Kv4.3 (33). NO can inhibit NMDA receptor currents through *S*-nitrosylation in the central nervous system (34), and mutating Cys-399 on the GluN2A subunit removes NO sensitivity (25). However, it has not been clear whether *S*-nitrosylation is involved in regulating N-type and P/Q-type Ca^{2+} channels by NO. In this study, we systematically determined the role of *S*-nitrosylation in the inhibition of HVA Ca^{2+} currents by NO. Compared with L-type and P/Q-type channels, N-type channels coassembled with Cav$\beta1$ or Cav$\beta3$ subunits

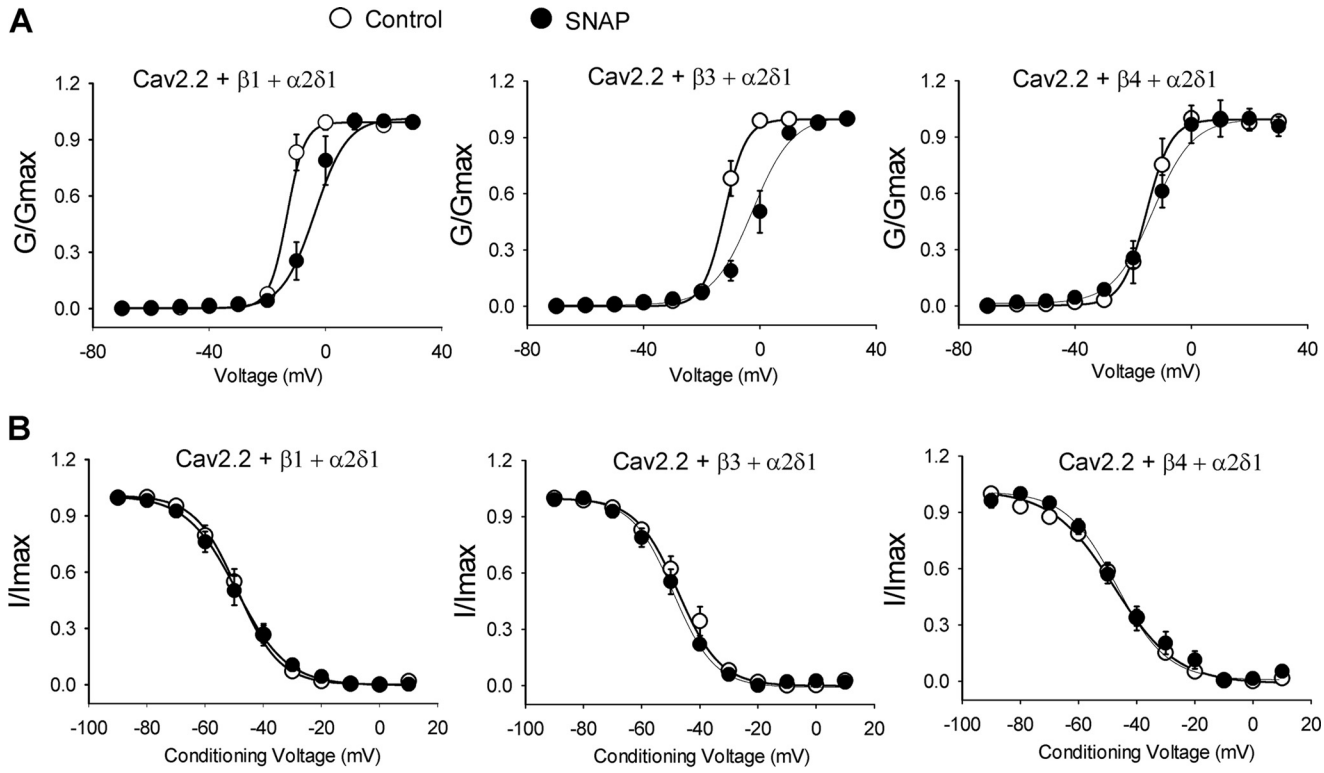

FIGURE 3. **Effect of SNAP on voltage-dependent activation and inactivation of N-type channels.** *A,* voltage-dependent activation curves of N-type channels reconstituted with Cav2.2, $\alpha_2\delta1$, and different Cavβ subunits. Voltage-dependent activation curves were obtained by plotting the normalized conductance as a function of the command potential recorded. *B,* voltage-dependent inactivation curves of N-type channels reconstituted with Cav2.2, $\alpha_2\delta1$, and different Cavβ subunits. Voltage-dependent inactivation curves were obtained using inactivation protocols. Data points were fitted using the Boltzmann equation. $V_{0.5}$ and slope factors are shown as the mean ± S.E. listed in Table 1.

TABLE 1

Effects of SNAP on the voltage-dependent activation and inactivation of N-type Ca^{2+} channels in HEK293 cells cotransfected with wild-type Cav2.2 (or Cav2.2 mutants), $\alpha_2\delta_1$, and Cavβ1, Cavβ3, or Cavβ4 subunits

Specific subunit combination	$V_{0.5}$	Slope factor	*n*
Voltage-dependent activation			
Cav2.2 + $\beta1$ + $\alpha_2\delta_1$	−13.23 ± 2.04	3.03 ± 0.91	9
Cav2.2 + $\beta1$ + $\alpha_2\delta_1$ (+SNAP)	−3.68 ± 4.68[a]	5.58 ± 1.54[a]	8
Cav2.2 + $\beta3$ + $\alpha_2\delta_1$	−12.13 ± 2.53	3.69 ± 1.16	8
Cav2.2 + $\beta3$ + $\alpha_2\delta_1$ (+SNAP)	−2.48 ± 1.72[a]	6.85 ± 0.80[a]	8
Cav2.2 + $\beta4$ + $\alpha_2\delta_1$	−15.44 ± 2.06	5.23 ± 0.71	8
Cav2.2 + $\beta4$ + $\alpha_2\delta_1$ (+SNAP)	−13.20 ± 1.48	6.84 ± 0.79	9
Cav2.2 C805A + $\beta3$ + $\alpha_2\delta_1$	−8.89 ± 2.42	5.29 ± 0.50	8
Cav2.2 C805A + $\beta3$ + $\alpha_2\delta_1$ (+SNAP)	−9.49 ± 4.21	7.06 ± 0.64	8
Cav2.2 C930A + $\beta3$ + $\alpha_2\delta_1$	−1.07 ± 2.32	3.55 ± 0.57	7
Cav2.2 C930A + $\beta3$ + $\alpha_2\delta_1$ (+SNAP)	−1.40 ± 3.84	5.74 ± 0.44	7
Voltage-dependent inactivation			
Cav2.2 + $\beta1$ + $\alpha_2\delta_1$	−48.94 ± 1.16	7.27 ± 0.52	8
Cav2.2 + $\beta1$ + $\alpha_2\delta_1$ (+SNAP)	−49.19 ± 1.04	8.63 ± 0.53	9
Cav2.2 + $\beta3$ + $\alpha_2\delta_1$	−47.45 ± 1.05	7.23 ± 0.45	8
Cav2.2 + $\beta3$ + $\alpha_2\delta_1$ (+SNAP)	−51.42 ± 0.89	6.68 ± 0.59	7
Cav2.2 + $\beta4$ + $\alpha_2\delta_1$	−47.73 ± 1.04	10.69 ± 0.86	8
Cav2.2 + $\beta4$ + $\alpha_2\delta_1$ (+SNAP)	−46.84 ± 1.77	8.72 ± 1.55	8
Cav2.2 C805A + $\beta3$ + $\alpha_2\delta_1$	−55.21 ± 0.60	11.30 ± 0.54	8
Cav2.2 C805A + $\beta3$ + $\alpha_2\delta_1$ (+SNAP)	−56.15 ± 0.76	11.16 ± 0.62	8
Cav2.2 C930A + $\beta3$ + $\alpha_2\delta_1$	−47.78 ± 1.53	9.89 ± 1.17	7
Cav2.2 C930A + $\beta3$ + $\alpha_2\delta_1$ (+SNAP)	−48.93 ± 1.07	11.83 ± 0.92	7

[a] $p < 0.05$, compared with the corresponding control (before SNAP application).

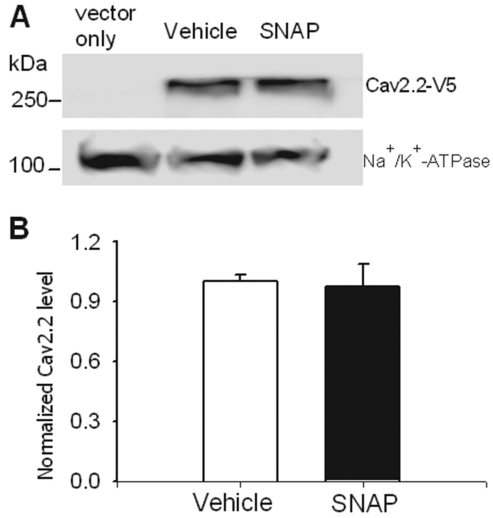

FIGURE 4. **SNAP does not affect Cav2.2 membrane surface expression.** *A,* original gel image shows the Cav2.2 protein levels on the membrane surface. For the vector-only group, HEK293 cells were cotransfected with pcDNA6 V5-FLAG vector + Cav$\beta3$ + $\alpha_2\delta1$ and were used as a blank control; for the SNAP group, HEK293 cells were cotransfected with Cav2.2-V5 + Cav$\beta3$ + $\alpha_2\delta1$ and treated with 100 μM SNAP for 5 min before cell surface biotinylation. *B,* summary data show that SNAP had no significant effect on the surface protein levels of Cav2.2-V5 ($n = 4$ independent experiments). The amounts of Cav2.2 proteins were normalized by Na^+/K^+-ATPase proteins on the same gel. The mean value of Cav2.2 treated with the vehicle was defined as 1.

showed prominent sensitivity to NO. The NO donor SNAP rapidly inhibited HVA Ca^{2+} currents, and this effect was readily reversed by DTT. Also, SNAP failed to inhibit HVA Ca^{2+} currents in the presence of MTSEA, which covalently modifies protein sulfhydryl groups. The sulfhydral side chain (-SH) of cysteine forms a covalent disulfide bond with sulfur in MTSEA (35), and this chemical reaction can prevent subsequent *S*-nitrosylation by NO. Notably, the modification by MTSEA does not affect ion channel function if the exposure time is less than 8 min (25, 29, 36). These findings demonstrate that N-type

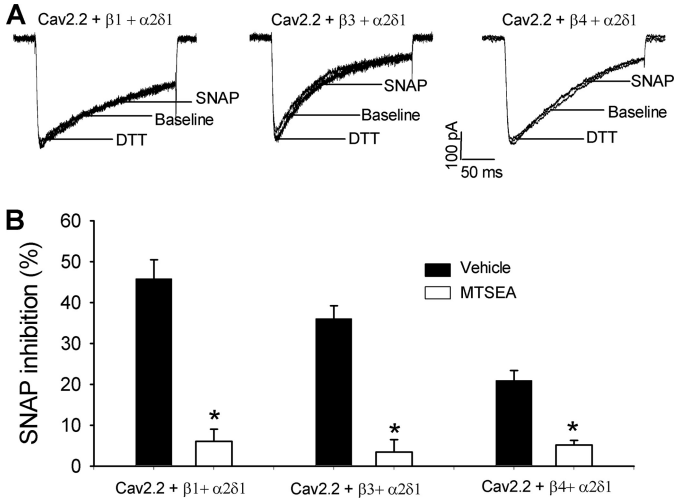

FIGURE 5. **MTSEA blocks the inhibitory effect of SNAP on N-type channels.** *A,* original current traces show the SNAP effects on N-type channels reconstituted with Cav2.2 + $\alpha_2\delta1$ and Cavβ1, Cavβ3, or Cavβ4 subunits in HEK293 cells. The cells were pre-treated with 2.5 mM MTSEA for 1 min before the whole cell recording. *B,* summary data show that MTSEA pre-treatment blocked the inhibitory effect of 100 μM SNAP on N-type channels. *, $p < 0.05$, compared with the vehicle control.

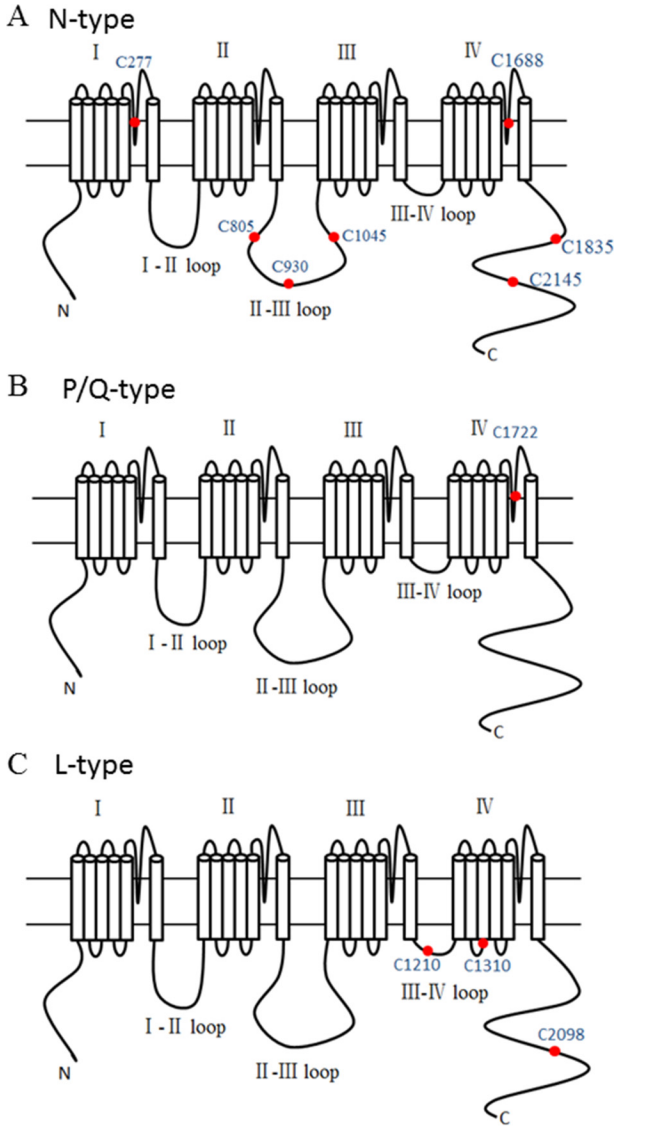

FIGURE 6. **Consensus motif positions of *S*-nitrosylation in Cavα_1 subunits.** *A,* the *red dots* in the diagrams denote the positions of the seven consensus motifs of *S*-nitrosylation in the N-type Cavα_1 subunit. *B,* the *red dot* shows the only consensus motif of *S*-nitrosylation in the P/Q-type subunit. *C,* the *red dots* indicate the positions of the three consensus motifs of *S*-nitrosylation in the L-type subunit.

channels with Cavβ1 or Cavβ3 subunits are particularly sensitive to NO via *S*-nitrosylation modulation.

We found that in N-type channels co-assembled with Cavβ1 or Cavβ3 subunits, the inhibitory effect of SNAP was associated with a significant depolarizing shift of voltage-dependent activation of N-type channels. However, SNAP treatment had no significant effect on the Cav2.2 protein abundance of the membrane surface. Cavβ subunits are critical for channel trafficking and surface expressions (1, 3). The trafficking of Ca^{2+} channels is controlled by numerous processes, including co-assembly with auxiliary subunits, ubiquitin ligases, and interactions with other membrane proteins (37). Ca^{2+} channel trafficking typically takes more than 10 min and does not change the channel kinetic properties (38, 39). Because the inhibitory effect of SNAP on HVA Ca^{2+} channels occurred rapidly and associated with the depolarizing shift of channel activations (*i.e.* reduced voltage-dependent activation) in our study, NO likely inhibits N-type Ca^{2+} channels through *S*-nitrosylation-induced changes in channel conformation and gating properties. Also, because SNAP failed to alter voltage-dependent activation of N-type channels when cysteine *S*-nitrosylation sites (*i.e.* C805A and C930A mutants) were mutated, our data suggest that the shift in voltage dependence likely accounts for all of the inhibitory effect of NO on N-type channels.

In this study, we also identified key structural motifs essential for the inhibitory gating of N-type Ca^{2+} channels via cysteine *S*-nitrosylation. Sequence alignment analysis indicated that the consensus motifs of *S*-nitrosylation are much more abundant in Cav2.2 than in Cav1.2 and Cav2.1. This structural distinction is consistent with our recording data showing that SNAP had a much more pronounced effect on N-type channels than on P/Q-type and L-type channels. Thus, the prominent sensitivity to NO is a characteristic of N-type channels. We found that several intracellular cysteine residues, including Cys-805 and Cys-930 in the II-III loop and Cys-1835 and Cys-2145 in the C terminus, critically mediate the *S*-nitrosylation modification of the N-type channels. Mutating Cys-1045 in the II-III loop also significantly reduced NO sensitivity of N-type channels. In concord with our findings, polynitrosylation modification is known to contribute to the activation of the ryanodine receptor (40). Multiple consensus motifs of *S*-nitrosylation also exist in NMDA receptors (25). The cytoplasmically accessible cysteine sites may produce an additive effect and transmit cysteine modifications to functionally critical domains of N-type channels to elicit their conformational changes. In addition, site-directed mutagenesis analysis showed that mutating Cys-346 of the Cavβ3 subunit decreased the NO inhibitory effect by ~50% compared with the wild-type Cavβ3. These data indicate that in addition to Cavα_1 subunits, the Cavβ subunit is also involved in redox modification of the N-type channel by NO. Our findings indicate that polynitrosylation modification is an important

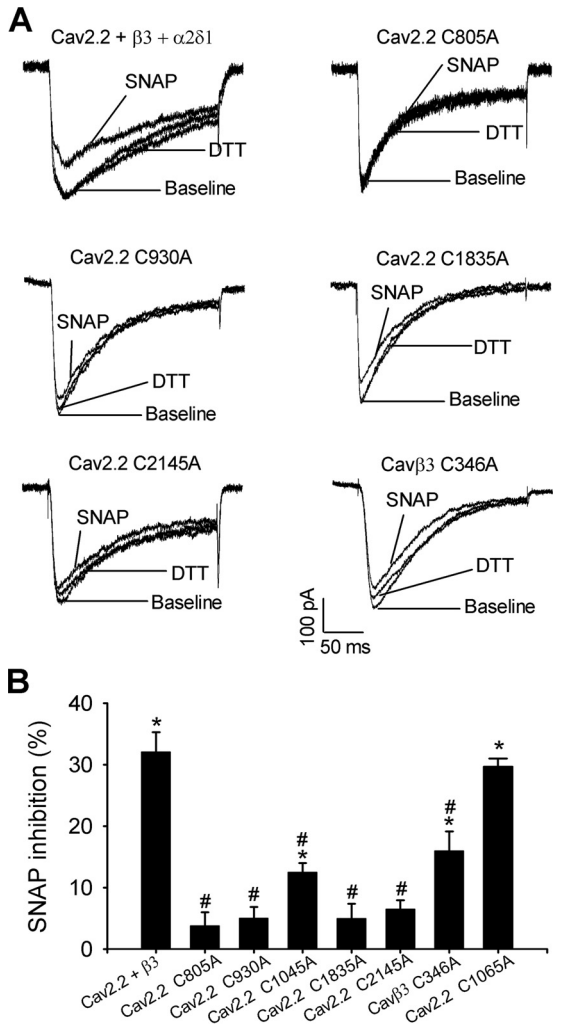

FIGURE 7. **Critical cysteine residues involved in *S*-nitrosylation control of N-type channels.** *A,* original current traces show the SNAP effects on N-type channel currents reconstituted with wild-type Cav2.2, Cavβ3, and their mutants in HEK293 cells. *B,* summary data show the effect of SNAP on N-type channel currents reconstituted with wild-type Cav2.2, Cavβ3, and their mutants. The percentage of inhibition of N-type channels by SNAP is shown as the mean ± S.E. in Table 2. *, $p < 0.05$, compared with the baseline control. #, $p < 0.05$, compared with wild-type controls.

TABLE 2

Inhibitory effects of SNAP on N-type Ca^{2+} channels reconstituted in HEK293 cells expressing wild-type Cav2.2, and Cavβ3 or their mutants

Specific subunit combination	SNAP inhibition	*n*
	%	
Wild-type Cav2.2 + $\beta3$ + $\alpha_2\delta_1$	32.09 ± 3.21[a]	7
Cav2.2 C805A + $\beta3$ + $\alpha_2\delta_1$	3.80 ± 2.17[b]	10
Cav2.2 C930A + $\beta3$ + $\alpha_2\delta_1$	5.05 ± 1.79[b]	7
Cav2.2 C1045A + $\beta3$ + $\alpha_2\delta_1$	12.53 ± 1.50[a,b]	7
Cav2.2 C1065A + $\beta3$ + $\alpha_2\delta_1$	29.75 ± 1.31[a]	6
Cav2.2 C1835A + $\beta3$ + $\alpha_2\delta_1$	5.00 ± 2.36[b]	6
Cav2.2 C2145A + $\beta3$ + $\alpha_2\delta_1$	6.54 ± 1.39[b]	8
Cav2.2 + $\beta3$ C346A + $\alpha_2\delta_1$	16.02 ± 3.13[a,b]	8

[a] $p < 0.05$, compared with the baseline current amplitude.
[b] $p < 0.05$, compared with the wild-type controls.

feature in the negative feedback regulation of N-type channels by NO.

In summary, our study provides new information for our understanding of HVA Ca^{2+} channel regulation by *S*-nitrosylation at the molecular level. Our findings reveal that cytoplasmically accessible cysteine residues serve as "NO sensors"

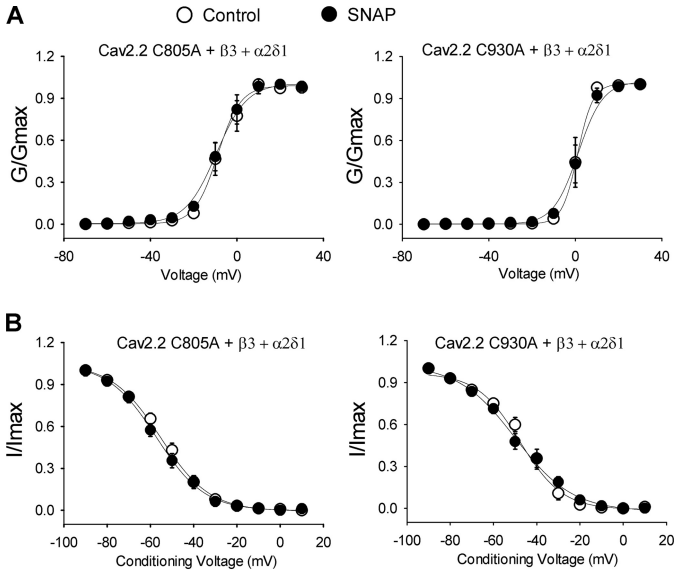

FIGURE 8. **Effect of SNAP on voltage-dependent activation and inactivation of N-type currents reconstituted with Cav2.2 mutants.** *A,* voltage-dependent activation curves of N-type channels reconstituted with C805A or C930A, Cavβ3, and $\alpha_2\delta1$ subunits. Voltage-dependent activation curves were obtained by plotting the normalized conductance as a function of the command potential. *B,* voltage-dependent inactivation curves of N-type currents reconstituted with C805A or C930A, Cavβ3, and $\alpha_2\delta1$ subunits. Voltage-dependent inactivation curves were obtained using inactivation protocols. Data points were fitted using the Boltzmann equation. $V_{0.5}$ and slope factors are shown as the mean ± S.E. listed in Table 1.

of HVA Ca^{2+} channels. This mechanism is important for the feedback regulation of Ca^{2+} signals by NO in neurons. N-type channels are expressed at high levels in both DRG neurons and their presynaptic terminals and are critically involved in triggering the neurotransmitter release from primary afferent terminals (9, 10, 41). N-type Ca^{2+} channels are also recognized as a crucial target for treating painful conditions. Both Cav2.2 and Cavβ3 subunits whose cysteine residues undergo *S*-nitrosylation probably conduct NO-induced inhibition of N-type channels in native DRG neurons. Thus, *S*-nitrosylation may play a critical role in feedback regulation of N-type channels by NO following stimulation of endogenous neuronal NO synthase in native primary sensory neurons (21, 24). The *S*-nitrosylation sites on N-type channels could be targeted for pain treatment.

Author Contributions—M. H. Z. and H. L. P. participated in research design. M. H. Z. and A. B. conducted experiments. M. H. Z. and H. L. P. performed data analysis. M. H. Z. and H. L. P. wrote the manuscript.

Acknowledgments—We thank Drs. Diane Lipscombe, Terrance P. Snutch, and Jiusheng Yan for providing Ca^{2+} channel cDNAs and vectors used in our study.

References

1. Catterall, W. A. (2000) Structure and regulation of voltage-gated Ca^{2+} channels. *Annu. Rev. Cell Dev. Biol.* **16,** 521–555
2. Catterall, W. A., and Few, A. P. (2008) Calcium channel regulation and presynaptic plasticity. *Neuron* **59,** 882–901
3. Buraei, Z., and Yang, J. (2010) The beta subunit of voltage-gated Ca^{2+} channels. *Physiol. Rev.* **90,** 1461–1506
4. Chen, Y. H., Li, M. H., Zhang, Y., He, L. L., Yamada, Y., Fitzmaurice, A.,

Shen, Y., Zhang, H., Tong, L., and Yang, J. (2004) Structural basis of the $\alpha 1$-β subunit interaction of voltage-gated Ca^{2+} channels. *Nature* **429,** 675–680
5. Gilbert, M., Jung, S. R., Reed, B. J., and Sweet, I. R. (2008) Islet oxygen consumption and insulin secretion tightly coupled to calcium derived from L-type calcium channels but not from the endoplasmic reticulum. *J. Biol. Chem.* **283,** 24334–24342
6. Urbano, F. J., Depetris, R. S., and Uchitel, O. D. (2001) Coupling of L-type calcium channels to neurotransmitter release at mouse motor nerve terminals. *Pflugers Arch.* **441,** 824–831
7. Filloux, F., Karras, J., Imperial, J. S., Gray, W. R., and Olivera, B. M. (1994) The distribution of ω-conotoxin MVIICnle-binding sites in rat brain measured by autoradiography. *Neurosci. Lett.* **178,** 263–266
8. Wu, Z. Z., Chen, S. R., and Pan, H. L. (2004) Differential sensitivity of N- and P/Q-type Ca^{2+} channel currents to a mu opioid in isolectin B4-positive and -negative dorsal root ganglion neurons. *J. Pharmacol. Exp. Ther.* **311,** 939–947
9. Wu, Z. Z., and Pan, H. L. (2004) High voltage-activated Ca^{2+} channel currents in isolectin B(4)-positive and -negative small dorsal root ganglion neurons of rats. *Neurosci. Lett.* **368,** 96–101
10. Murali, S. S., Napier, I. A., Rycroft, B. K., and Christie, M. J. (2012) Opioid-related (ORL1) receptors are enriched in a subpopulation of sensory neurons and prolonged activation produces no functional loss of surface N-type calcium channels. *J. Physiol.* **590,** 1655–1667
11. Nimmervoll, B., Flucher, B. E., and Obermair, G. J. (2013) Dominance of P/Q-type calcium channels in depolarization-induced presynaptic FM dye release in cultured hippocampal neurons. *Neuroscience* **253,** 330–340
12. Robbe, D., Alonso, G., Chaumont, S., Bockaert, J., and Manzoni, O. J. (2002) Role of P/Q-Ca^{2+} channels in metabotropic glutamate receptor 2/3-dependent presynaptic long-term depression at nucleus accumbens synapses. *J. Neurosci.* **22,** 4346–4356
13. Müller, C. S., Haupt, A., Bildl, W., Schindler, J., Knaus, H. G., Meissner, M., Rammner, B., Striessnig, J., Flockerzi, V., Fakler, B., and Schulte, U. (2010) Quantitative proteomics of the Cav2 channel nano-environments in the mammalian brain. *Proc. Natl. Acad. Sci. U.S.A.* **107,** 14950–14957
14. Luvisetto, S., Marinelli, S., Panasiti, M. S., D'Amato, F. R., Fletcher, C. F., Pavone, F., and Pietrobon, D. (2006) Pain sensitivity in mice lacking the $Ca_v2.1\alpha 1$ subunit of P/Q-type Ca^{2+} channels. *Neuroscience* **142,** 823–832
15. Saegusa, H., Kurihara, T., Zong, S., Kazuno, A., Matsuda, Y., Nonaka, T., Han, W., Toriyama, H., and Tanabe, T. (2001) Suppression of inflammatory and neuropathic pain symptoms in mice lacking the N-type Ca^{2+} channel. *EMBO J.* **20,** 2349–2356
16. Cao, X. H., Byun, H. S., Chen, S. R., and Pan, H. L. (2011) Diabetic neuropathy enhances voltage-activated Ca^{2+} channel activity and its control by M4 muscarinic receptors in primary sensory neurons. *J. Neurochem.* **119,** 594–603
17. Li, L., Cao, X. H., Chen, S. R., Han, H. D., Lopez-Berestein, G., Sood, A. K., and Pan, H. L. (2012) Up-regulation of Cavβ3 subunit in primary sensory neurons increases voltage-activated Ca^{2+} channel activity and nociceptive input in neuropathic pain. *J. Biol. Chem.* **287,** 6002–6013
18. Hall, K. E., Sima, A. A., and Wiley, J. W. (1995) Voltage-dependent calcium currents are enhanced in dorsal root ganglion neurones from the Bio Bred/Worchester diabetic rat. *J Physiol.* **486**, 313–322
19. Chen, X., and Levine, J. D. (1999) NOS inhibitor antagonism of PGE_2-induced mechanical sensitization of cutaneous C-fiber nociceptors in the rat. *J. Neurophysiol.* **81,** 963–966
20. Guan, Y., Yaster, M., Raja, S. N., and Tao, Y. X. (2007) Genetic knockout and pharmacologic inhibition of neuronal nitric-oxide synthase attenuate nerve injury-induced mechanical hypersensitivity in mice. *Mol. Pain* **3,** 29
21. Bavencoffe, A., Chen, S. R., and Pan, H. L. (2014) Regulation of nociceptive transduction and transmission by nitric oxide. *Vitam. Horm.* **96,** 1–18
22. Hoheisel, U., Unger, T., and Mense, S. (2000) A block of spinal nitric oxide synthesis leads to increased background activity predominantly in nociceptive dorsal horn neurones in the rat. *Pain* **88,** 249–257
23. Zhuo, M., Meller, S. T., and Gebhart, G. F. (1993) Endogenous nitric oxide is required for tonic cholinergic inhibition of spinal mechanical transmission. *Pain* **54,** 71–78
24. Jin, X. G., Chen, S. R., Cao, X. H., Li, L., and Pan, H. L. (2011) Nitric oxide inhibits nociceptive transmission by differentially regulating glutamate and glycine release to spinal dorsal horn neurons. *J. Biol. Chem.* **286,** 33190–33202
25. Choi, Y. B., Tenneti, L., Le, D. A., Ortiz, J., Bai, G., Chen, H. S., and Lipton, S. A. (2000) Molecular basis of NMDA receptor-coupled ion channel modulation by *S*-nitrosylation. *Nat. Neurosci.* **3,** 15–21
26. Kakizawa, S., Yamazawa, T., Chen, Y., Ito, A., Murayama, T., Oyamada, H., Kurebayashi, N., Sato, O., Watanabe, M., Mori, N., Oguchi, K., Sakurai, T., Takeshima, H., Saito, N., and Iino, M. (2012) Nitric oxide-induced calcium release via ryanodine receptors regulates neuronal function. *EMBO J.* **31,** 417–428
27. Li, L., Li, D. P., Chen, S. R., Chen, J., Hu, H., and Pan, H. L. (2014) Potentiation of high voltage-activated calcium channels by 4-aminopyridine depends on subunit composition. *Mol. Pharmacol.* **86,** 760–772
28. Wu, Z. Z., Li, D. P., Chen, S. R., and Pan, H. L. (2009) Aminopyridines potentiate synaptic and neuromuscular transmission by targeting the voltage-activated calcium channel β subunit. *J. Biol. Chem.* **284,** 36453–36461
29. Hu, H., Chiamvimonvat, N., Yamagishi, T., and Marban, E. (1997) Direct inhibition of expressed cardiac L-type Ca^{2+} channels by *S*-nitrosothiol nitric oxide donors. *Circ. Res.* **81,** 742–752
30. Stamler, J. S., Toone, E. J., Lipton, S. A., and Sucher, N. J. (1997) (S)NO signals: translocation, regulation, and a consensus motif. *Neuron* **18,** 691–696
31. Hess, D. T., Matsumoto, A., Kim, S. O., Marshall, H. E., and Stamler, J. S. (2005) Protein *S*-nitrosylation: purview and parameters. *Nat. Rev. Mol. Cell Biol.* **6,** 150–166
32. Jaffrey, S. R., Erdjument-Bromage, H., Ferris, C. D., Tempst, P., and Snyder, S. H. (2001) Protein *S*-nitrosylation: a physiological signal for neuronal nitric oxide. *Nat. Cell. Biol.* **3,** 193–197
33. Gonzalez, D. R., Treuer, A., Sun, Q. A., Stamler, J. S., and Hare, J. M. (2009) *S*-Nitrosylation of cardiac ion channels. *J. Cardiovasc. Pharmacol.* **54,** 188–195
34. Hopper, R., Lancaster, B., and Garthwaite, J. (2004) On the regulation of NMDA receptors by nitric oxide. *Eur. J. Neurosci.* **19,** 1675–1682
35. Holmgren, M., Liu, Y., Xu, Y., and Yellen, G. (1996) On the use of thiol-modifying agents to determine channel topology. *Neuropharmacology* **35,** 797–804
36. O'Reilly, J. P., and Shockett, P. E. (2012) Time- and state-dependent effects of methanethiosulfonate ethylammonium (MTSEA) exposure differ between heart and skeletal muscle voltage-gated Na^+ channels. *Biochim. Biophys. Acta* **1818,** 443–447
37. Simms, B. A., and Zamponi, G. W. (2012) Trafficking and stability of voltage-gated calcium channels. *Cell Mol. Life Sci.* **69,** 843–856
38. Hendrich, J., Van Minh, A. T., Heblich, F., Nieto-Rostro, M., Watschinger, K., Striessnig, J., Wratten, J., Davies, A., and Dolphin, A. C. (2008) Pharmacological disruption of calcium channel trafficking by the $\alpha 2\delta$ ligand gabapentin. *Proc. Natl. Acad. Sci. U.S.A.* **105,** 3628–3633
39. Altier, C., Dubel, S. J., Barrère, C., Jarvis, S. E., Stotz, S. C., Spaetgens, R. L., Scott, J. D., Cornet, V., De Waard, M., Zamponi, G. W., Nargeot, J., and Bourinet, E. (2002) Trafficking of L-type calcium channels mediated by the postsynaptic scaffolding protein AKAP79. *J. Biol. Chem.* **277,** 33598–33603
40. Xu, L., Eu, J. P., Meissner, G., and Stamler, J. S. (1998) Activation of the cardiac calcium release channel (ryanodine receptor) by poly-*S*-nitrosylation. *Science* **279,** 234–237
41. Bao, J., Li, J. J., and Perl, E. R. (1998) Differences in Ca^{2+} channels governing generation of miniature and evoked excitatory synaptic currents in spinal laminae I and II. *J. Neurosci.* **18,** 8740–8750